Spring 4-29-2022

Development of a New Method for Cell Spheroid Formation Through a Hydrogel Dipping Process

Aimee L. Co
aimee.co@maine.edu

DEVELOPMENT OF A NEW METHOD FOR CELL SPHEROID FORMATION THROUGH A HYDROGEL DIPPING PROCESS

By

Aimee Co

B.A. University of Maine, 2015

A Thesis

Submitted in Partial Fulfillment of the

Requirements for the Degree of

Master of Science

(in Biomedical Engineering)

The Graduate School

The University of Maine

May 2022

Advisory Committee:

Dr. Thomas J. Schwartz, Associate Professor of Chemical and Biomedical Engineering, Advisor

Dr. Michael D. Mason, Professor of Chemical and Biomedical Engineering

Dr. Karissa Tilbury, Assistant Professor of Chemical and Biomedical Engineering

Dr. Bashir Khoda, Assistant Professor of Mechanical Engineering

DEVELOPMENT OF A NEW METHOD FOR CELL SPHEROID FORMATION THROUGH A HYDROGEL DIPPING PROCESS

By Aimee Co

Thesis Advisor: Dr. Thomas J. Schwartz

An Abstract of the Thesis Presented
In Partial Fulfillment of the Requirements for the
Degree of Master of Science
(in Biomedical Engineering)
May 2022

Traditional cell culture systems make use of two-dimensional (2D) monolayer studies which are simple, cheap, and have been successful for a various cell types. However, since this does not reflect on the *in vivo* physiology, studies have branched out to use three-dimensional (3D) cell culture systems. 3D cell culture allows for studies which make use of the cell connectivity, polarity, and tissue architecture. The use of 3D aggregates called spheroids is one of the most common and versatile of these methods. There are various techniques for spheroid formation and chosen technique is often decided based on the decided spheroid use and size. Many of these methods are limited by the quantity, size, and reproducibility of the spheroids. A new method focused on the manufacturability of the process would overcome these issues. By focusing on the manufacturability of the process, spheroids would be able to be produced in larger quantities and consistently sized.

The goal of this study is to manufacture and characterize droplet-on-fiber through a dipping process. The withdrawal of the fiber from a liquid solution will result in a coating due to the balance between the viscous drag and the capillary rise. The thickness of the layer depends upon various parameters of the fluid and dipping process. Above a threshold coating thickness, Rayleigh-Plateau Instability will trigger the formation of droplets. Controlling the process

parameters will determine the liquid volume in the droplet and its morphology. Such a simple droplet formation technique will be less resource intensive than existing methods and can produce droplets of various sizes and shapes in a short amount of time.

Extruded polylactic acid (PLA) fiber is considered as the substrate for droplet adherence while alginate solution is used for the dipping fluid. The focus of this work is on the shape fidelity and reproducibility of the droplet formation by varying the dipping fluid composition. The aspect ratio between droplet diameter and wetting length is defined as a quantifiable shape-fidelity index which is reported in this work. By varying the dipping fluid composition, the relationship between the viscosity of the dipping fluid (alginate) and the PLA fiber can be identified. The observations made throughout this thesis will allow for further development of this dipping process, as well as determine the optimal concentration of alginate to achieve reproducible droplets with the desired morphology for cell spheroid formation.

ACKNOWLEDGEMENTS

I would like to thank my committee, Dr. Thomas J. Schwartz, Dr. Michael D. Mason, Dr. Karissa Tilbury, and Dr. Bashir Khoda for all the help you have given during this project and composition of this thesis. I have been able to learn a large amount of skill throughout my time at UMaine which I'm sure will help me in the future. A big thank you to the Mason Lab group graduate students, both past and present. Of them I would specifically like to thank Dr. Ania Sitarski, Dr. Radowan Hossen, David Hollomakoff, Jeremy Grant, and Mitchell Chesley, who gave me a great deal of knowledge and guidance, even when I didn't know I needed it. I would like to thank Madison Mueth, a fellow graduate student that helped a great deal with this research within the short time span of her rotation at UMaine.

Finally, I would like to thank my family for being my support system throughout my school career. Thank you to my mom and my sister Audrey, for all of your support and being able to keep me on track and awake in my early graduate years. Thank you to my dad for being my source of fluid dynamics knowledge as well as overall graduate school knowledge. And a big thank you to my sister Aileen, who has worked in the same lab as me this entire time and has helped me both in school and at home.

TABLE OF CONTENTS

LIST OF TABLES

LIST OF FIGURES

CHAPTER 1

INTRODUCTION AND BACKGROUND

1.1 3D cell culture and importance in spheroid creation

General knowledge on cellular processes is derived from experiments using cells cultured on two-dimensional (2D) surfaces. Two-dimensional cell culture involves the plating of either primary cells directly from tissue, or a secondary cell line which has been immortalized. These culture systems are often used for *in vitro* tissue studies and will generally use cells which will adhere to the bottom of the cell culture plate or flask they have been place within. Two-dimensional cell culture systems form in a monolayer and create a well-controlled and homogenous cell environment (Figure 1.1). This type of system is ideal for studies that require sustained cell proliferation, high reproducibility, and easy maintenance. Since 2D culture is extremely common, supplies for maintenance and testing are commercially available and less expensive than alternatives.

However, while these 2D cell culture systems have the advantage of being simple, cheap, and successful for a variety of cell types, they do not reflect the *in vivo* physiology [1-6]. Adherent cells will proliferate when plated in the correct conditions but are limited to a monolayer formation due to the space constrictions of the container. The lack of tissue-specific architecture, cell-to-cell and cell-to-matrix connections can have an effect on the cell proliferation, function, and response to external stimuli [2-4, 7]. For example, when primary hepatocytes are taken out of the body and put into 2D culture, they rapidly lose their normal phenotype. However, this loss can be reduced or even reversed through use of three dimensional (3D) culture methods[2].

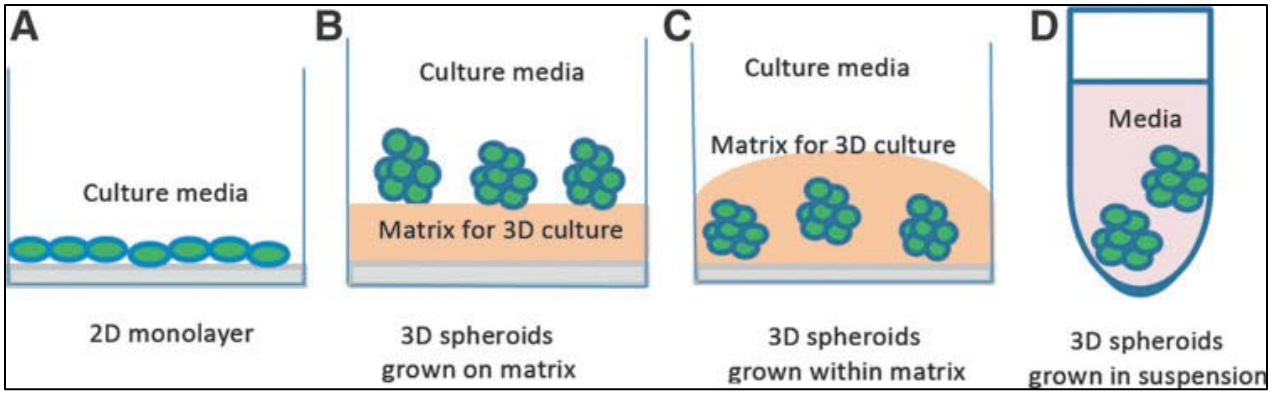

Figure1.1: Diagram showing the difference between the different cell culture systems. An example of a typical 2D cell culture(A) is shown alongside the different variations of 3D cell culture (B-C) [5]

The use of three-dimensional cell culture systems gives the ability to represent the *in vivo* morphology and makes use of the cell connectivity, polarity, gene expression, and tissue architecture. One of the most common and versatile methods of 3D cell culture are three-dimensional aggregates called spheroids. The use of spheroids has been adapted for cell traditionally cultured in 2D and so has been found extremely useful for various applications. A spheroid culture system has been found to be ideal for applications such as the use of mesenchymal stem cells (MSCs) in transplantation therapy since differentiation of MSCs is enhanced within the spheroid culture system[3]. The concept for the use of spheroids is based on the physical and biochemical features of a tissue mass. A well-known usage of spheroid cell culture is for the modeling of tumors since this structure allows for variable availability of essential compounds such as oxygen and nutrient similar to an *in vivo* environment. These include studies on metastatic processes, as well as drug testing, and cell responses to irradiation [1].

1.2 Current methods and problems

Spheroid formation techniques can be split into two general categories: 1) scaffold-based techniques and 2) scaffold-free techniques [5, 6, 8]. The difference between the usages of these two categories depends on the type of cells, tissue origin, and the need for high throughput capabilities. Scaffold-based techniques mimic the extracellular matrix which can be composed of

either biological or synthetic materials with varying porosity, permeability, surface chemistry, and stiffness to replicate the microenvironment of specific tissues. One such scaffold is a hydrogel. Hydrogels are commonly used in cell culture studies since these materials have the ability to entrap cells in an environment similar to the extracellular matrix and have been shown to improve the viability, differentiation, and angiogenetic capacity of stem cells.

Scaffold-free techniques promote cell-to-cell adhesion over cell-to-surface adhesion and so use a forced self-assembly process which more accurately replicates events that occur *in vivo*. Examples of this type of spheroid formation method include the hanging drop method, low cell attachment plates, spinner flasks, and microfluidics [2-4, 6, 9, 10]. While these methods are generally successful, they tend to vary in complexity and produce spheroids of different size and morphology. A comparison of these methods are given in Table 1.1. Spheroids have a multitude of applications, however, these methods are limited by the complexity, the range of spheroid sizes that can be produced, and reproducibility. The ability to generate consistent characteristics to spheroids in a less complex and quick manner would give the advantage of manufacturability. Current methods for spheroid formation which are able to be scaled up have presented disadvantages such as being unable to visualize the cells and causing damage to the cells.

Table 1.1: Various methods of spheroid formation [2-4, 6, 9, 10]

Method	**Pros**	**Cons**
Hanging Drop: • Relies on gravity-enforced self-assembly for spheroid production • 20-30μL of cell suspension used	• Multiple cell types can be co-cultured to create heterotypic spheroids. • Advanced into large production quantity.	• Difficult to track spheroids during formation • Non trivial to exchange media or add drugs

Table 1.1 continued

Spinner Culture: • Constant stirring of cells in suspension prevents settling and promotes cell-to-cell collisions	• Constant fluid movement aids in mass transport in and out of spheroids • Easy control of culture conditions • Has been scaled for large spheroid production	• Shear forces may damage cells with low cohesiveness, sensitive to shear forces. • If stir rate is too slow the cells can sink to the bottom of the container and inhibit spheroid formation • Cells are unable to be visualized due to constant mixing
Pellet culture: • Centrifugal force to concentrate cells at bottom of tube • Forms spheroids of fairly large diameter	• Simple and rapid • Large number of cells can aggregate	• Shear stress from centrifugation can damage cells • Cells not able to be visualized
Liquid Overlay: • Inhibits attachments to tissue culture plates by use of low-adhesive surfaces. • Plates rocked with a small amount of shaking.	• Simple • Allows for monitoring of individual spheroid formation and growth	• Spheroids often heterogeneous in both size and shape
Microfluidics: • Cells flow through microchannel network until partitioned and exposed to micro-rotational flow to cause aggregation.	• Allows for high throughput production • Good control of spheroid size	• Requires a technological capacity

1.3 Need for manufacturability

Manufacturability can generally be thought of the ease of which a product can be manufactured at a large scale and is determined by components such as production time,

production cost, and production volume. Design for Manufacture (DFM) is a practice that occurs early in the product development process which aims to optimize manufacturing time which results in reducing costs and increasing the ease of manufacturing. The important parameters that need to be considered for the manufacturability of the process is the speed, simplicity, consistency, availability of resources, the possibility of automation. These parameters gives the user full control over the results, making it easy to upscale.

Spheroid studies often require a large quantity of specific spheroid sizes to prove the reliability of the results. This is why a scalable process is important for spheroid development as this would increase the testing sizes as well as variation of trials whether the usage be for 3D structure development or drug trials. To be able to reach this goal, the manufacturability of the spheroid formation method should considered to produce a simple and quick process with reproducible results.

As mentioned above, an important parameter when looking at the manufacturability of a process is the speed. Any limitations to the speed of the process can be overcome through the use of automation which would make the process easy to control and produce consistent results. An important spheroid characteristic is the diameter which have a range of 200-600μm. The desired size of the spheroid is dependent on the types of cells used as well as the type of study [3, 4, 11, 12]. For example, spheroids for tumor studies are limited to no more than 500μm diameter as they undergo necrosis and have restricted nutrients, oxygen and growth factors similar to tumor cells[3]. The resulting sizes of the spheroids are restricted to the methods used for the formation and are hard to control, making this one of the main issues with current spheroid formation methods.

Entrapping cells in droplets of hydrogel in a simple and controlled manner would allow for production of consistently sized spheroids. This is similar to the known method of the hanging drop method which is a successful in producing a large quantity of spheroids of an adjustable size. However, this method has a disadvantage of being unable to track the formation as well as

difficulties exchanging media or adding drugs. The hanging drop method makes use of the media surface tension to keep the droplet structure hanging from the platform which means it needs to remain undisturbed. The use of a hydrogel-media mixture would give a droplet more structure and additional crosslinking may give the ability to submerge the droplet in media.

The automation of droplet formation can be achieved using a variety of methods, but it would be ideal to make use of existing machinery. Fiber dipping is a known method generally used for coating fibers with the goal of a smooth and even surface. The parameters are usually adjusted to avoid coating instabilities such as droplet formation so they can also be adjusted to promote droplet formation. An automated z-axis to control hydrogel droplet formation on a dipped fiber would be ideal for a proposed method for manufacturing spheroid formation

CHAPTER 2

METHODS AND MATERIALS

2.1 Proposed method

The current methods for spheroid formation are useful and successful but still have room for improvement. There are still limitations in large quantity spheroid reproducibility as well as issues such as cell damage and visibility. These are important issues as replicates are often needed in cell culture trials for thorough investigation. The development of a method for spheroid formation which focuses on manufacturability would put emphasis on a process which should have good reproducibility at large quantities.

The proposed method for a droplet formation process originates from the base idea of fluid coating, which is the simple operation of using movement to force a fluid to coat a solid. Fluid coatings can have various geometries such as plate coating, roll coatings, and fiber coatings. Fiber coatings are often achieved through a dipping process in which the fiber is dipped into a fluid then withdrawn so that a coating forms. In this case, rather than having the goal of a smooth fiber coating, the intended result would be an unstable fluid coating which would then break up into droplets on the fiber. The fluid would contain mammalian cells which would then be encased in the resulting droplets. Since there would be a lack of surfaces to adhere, the cells would instead adhere to each other to form spheroids.

2.2 Physics

The physics of this process can be described according to two phenomena. The first involves the fiber coating process and the second is the formation of the droplets from the fiber coating. The first step of the dipping process is the fiber coating of which the important parameters are the speed of the process and the fiber diameter. The rough assumption for the relationships within the process is that the thickness of the coating is a function of the velocity or dipping speed[13]. An important parameter is the capillary number (Ca):

$$Ca = \frac{\eta V}{\gamma}$$

where η is the fluid viscosity, V is the coating velocity, and γ is the surface tension. This is the ratio of the viscous and capillary forces which play antagonistic roles during the withdrawal process. As the solid lifts out of the fluid, the viscosity causes fluid near the fiber to move at the same velocity as the solid. This movement also causes a disruption to the liquid-air interface, working against the surface tension. This ratio is used for determining the coating thickness on the fiber which can be generally expressed as

$$h = \ell f(Ca)$$

where *h* is the coating thickness and ℓ is some static length which depends on the geometry of the solid. From this general form, various expressions have been determined such as the Landau, Levich, and Deraguin (LLD) theory which is written as

$$h = 1.34 r Ca^{\frac{2}{3}}$$

where r is the fiber radius. This equation is derived for small capillary numbers such that *h*<<*r* as it implies *Ca*<<*1.*

The derivation of the LLD theory neglects inertia due to small coating velocities. In the case that a low viscosity liquid is used to coat a fiber at large velocities, inertia becomes influential and can be evaluated using the Weber numb (*We*):

$$We = \frac{\rho V^2 r}{\gamma}$$

Where ρ is the fluid density. This value is used to compare the inertia with the capillary force. The use of higher velocities causes the kinetic energy to increase so the fluid close to the fiber becomes insensitive to the Laplace pressure trying to push the fluid back to the reservoir [13-15]. Larger velocities cause *We>1,* so the film thickness does not depend on the surface tension. This is based around a critical velocity which causes a sharp increase in film thickness and can be calculated by assuming *We=1*.

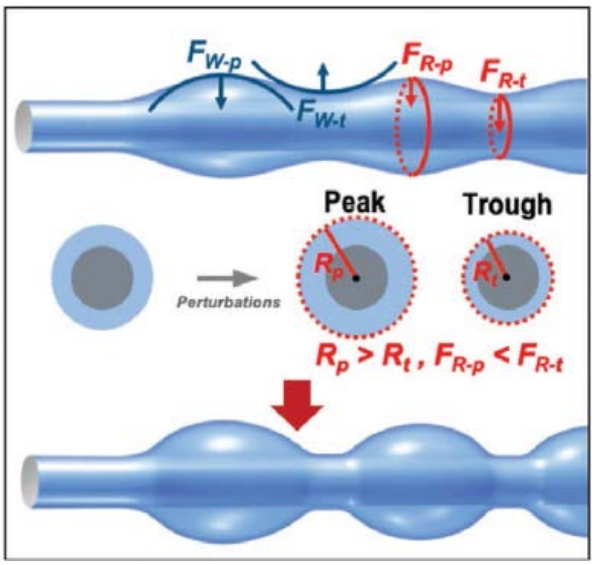

Figure 2.1: Visualization of Rayleigh-Plateau Instability[16]

The phenomenon that occurs after the coating step is the formation of droplets on the fiber caused by Rayleigh-Plateau Instability (RPI) [13, 16-21]. The progression of RPI originates from the idea that fluid streams will always have tiny perturbations present due to some external disturbance. Over time, the perturbations will increase and can be visualized as a series of sinusoidal components. The driving force in this phenomena is the Laplace pressure across a curved interface which produces an increased pressure inside a convex surface. This is represented in the Young-Laplace equation:

$$\Delta p = \alpha \left(\frac{1}{R_1} + \frac{1}{R_2} \right)$$

Where R_1 and R_2 are the principal radii of curvature. After the fiber coating, the presence of tiny perturbations creates regions of different thicknesses and therefore different Laplace pressures from the difference in the radius of curvature. This pressure difference promotes the instability growth which leads to the droplet formation.

This is visualized in Figure 2.1 where it's important to know that there are two radii components at play, the radius of the stream (F_R) and the radius of curvature of the wave itself (F_W). The transverse sections of the sinusoidal components show a growing radius at the peaks

(R_P) compared to the decaying trough regions (R_T). This means that the Laplace pressure towards the center of the peak (F_{R-p}) is smaller than at the trough (F_{R-t}). This generates a Laplace pressure difference (F_R) which pushes the liquid to move from the trough to the peak, increasing the instability. Simultaneously the radius component of the curvature of the wave itself generates a Laplace pressure difference (F_W) which is able to decrease the instability. F_{W-p} represents the areas of positive curvature while F_{W-t} represents the negative curvature. The radius of the stream (F_R) works against radius the curvature (F_W), and when the F_R acts dominantly, the sinusoidal components will grow to eventually initiate droplet formation [13, 16-18, 21].

2.3 Material Selection

The dipping fiber and fluid selection were among the first decisions that were needed for the development of the device. The initial considerations were heavily based on the known biocompatibility of the materials as this was an important characteristic for cell spheroid formation.

2.3.1 The Dipping Fluid

The chosen hydrogel for the project was alginate which is commonly used in biomaterial processes such as 3D bioprinting. This polysaccharide is generally obtained from brown algae and can become a hydrogel when the aqueous alginate solution is combined with an ionic crosslinking solution such as divalent cations such as Ca^{2+}.

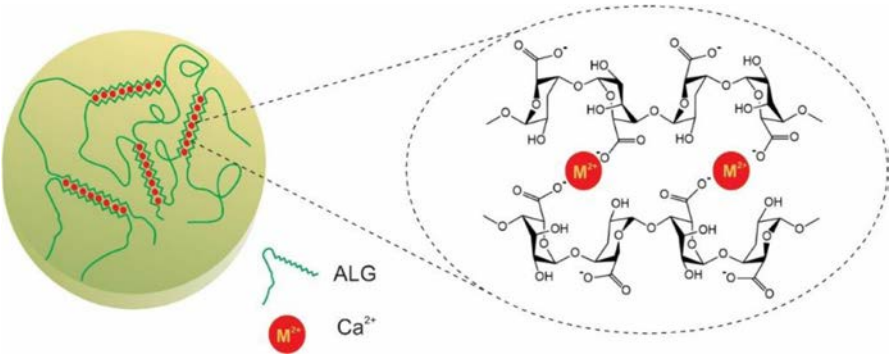

Figure 2.2: Alginate crosslinking [22]

It is believed that this occurs due to the interactions with the guluronate blocks of adjacent alginate chains, creating ionic bridges which forms the egg-box model of crosslinking (see Figure 2.2),

resulting in the gel structure [22-24]. This hydrogel was chosen due to its ease of use and availability.

2.3.2 The Fiber

Materials such as silk thread and metal wire were initially evaluated for use as dipping fiber. It was quickly decided that soft fibers such as cotton, silk, and hemp were not ideal as they would fold within the fluid during the dipping process and often would appear to absorb the fluid. Copper wires of various thicknesses were tested and were found to have the most consistent results of the initial materials tested. Although the droplets from the wire dipping were mostly consistent, some inconsistencies were still present due to the wires not being fully straight. The bulk wires were bought in a roll and so required a straightening process before usage which was unable to remove the bumps completely. The suggestion was made to use extruded PLA fibers as this was in abundant supply and the extrusion process would create a straight fiber.

Thus we tested extruded PLA fibers as they are known to be biocompatible and could be created at various diameters through the use of different extrusion nozzles ranging from 0.2mm to 1.0mm. This range was then narrowed down as it was found that the larger fiber diameters of 0.6mm and 1.0mm created extremely large droplets which would immediately fall off the fiber. The fiber diameter of 0.2mm produced the most consistent droplet size and quantity, and so was chosen to analyze the droplet shape fidelity and reproducibility by varying the dipping fluid concentration.

2.4 Material preparation

The alginate solution was prepared based on the desired mass concentration. The method for the calculation is as follows:

*Mass Concentration (g/mL) * DI Water (mL) = Alginate powder (g)*

Once the desired mass was calculated and measured, the volume of deionized water was measured and stirred with a magnetic stir-plate. While the water was being stirred the alginate powder (Sigma, Alginic acid sodium salt from brown algae) was slowly added to avoid clumping

then left to stir overnight. The alginate powder took a long time to dissolve in the DI water and so was left to stir overnight. The choice of stirring speed was dependent on the concentration of the material being prepared since the higher alginate concentrations such as 5-7 w/v% would create more viscous fluids and caused issues with the stir bar at higher speeds. This process was also repeated for the preparation of the calcium chloride solution (Sigma, Calcium chloride, anhydrous BioReagent).

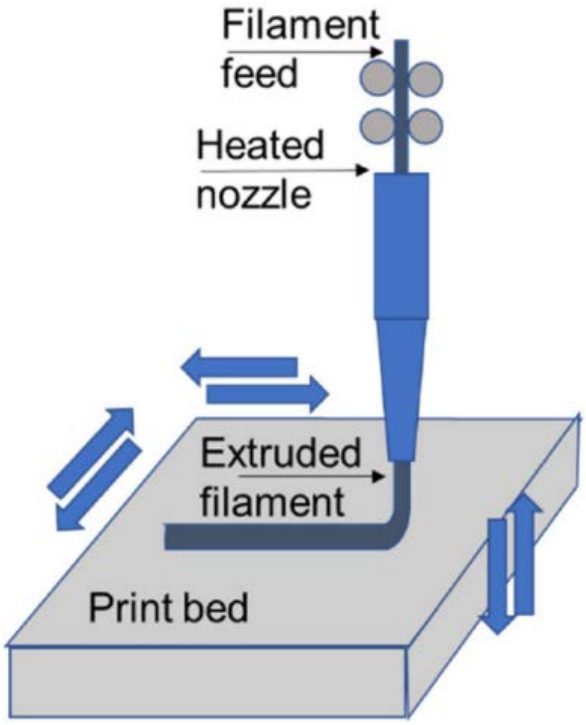

Figure 2.3: Example of general extrusion process used to make PLA fibers for dipping [25]. The PLA filament is fed from the bulk spool into the heated nozzle which melts and extrudes the material to result in the extruded fiber which is used for the dipping.

The fiber used in the dipping process was extruded PLA fiber. During this process, the 3D printing filament was steadily extruded through the nozzle of a 3D printer and constantly cut with scissors before the fiber reached the printer stage. Once removed from the moving extrusion filament the ends of the fiber were cut to avoid bent sections and the fiber diameter was checked with a caliper.

CHAPTER 3
PROCESS AND DEVICE DEVELOPMENT

3.1 Overall Criteria

While the overall goal is a scaled up process, the basic parameters must first be determined. The proposed idea for spheroid formation uses a fiber dipping process to create droplets which are to contain the cells for spheroid formation. This method requires the formation of a device which can control the fiber dipping process into the hydrogel fluid. Adjustments to the dipping speed should be available to control the droplet formation alongside the hydrogel concentration.

The device itself can be broken up into the basic sections of importance which fit the design criteria. The main source of control for the droplet formation is from the z-axis dipping motion since the droplets are dependent on the initial fluid coating. The second area of importance for the device design is the fluid containment. This is important for the volume of the fluid and the relation to potential cell containment within the droplets. A large cell concentration (cells/mL) would be ideal to increase the amount of cells which could be contained within the droplets. The T75 flasks used for cell culture have the ability to hold a confluency maximum of $8.4x10^6$ cells. Using this amount of cells as an example, this quantity within a small fluid volume would produce a high concentration which would increase the probability of cell containment within the droplets. The last physical aspect of the device design to be considered is the imaging of the droplets for analysis. The imaging results are used to measure the droplet dimensions which determine the effects of changes made to the process and device setup. The droplets are the product from the process and are observed as to whether they would be able to contain cells to form spheroids.

3.2 Z-axis Movement

The most important criteria for the design of the dipping device was the need for z-axis movement. The dipping movement is the action which causes the fluid to coat the fiber. While this

often occurs regardless of the parameters, this fiber coating thickness needs to be controlled to meet the requirements for Rayleigh-Plateau Instability to occur and form the droplets. This criteria went through the most changes over the development of the device as initial tests were done by hand before evolving into a useful machine of which the dipping height and speed could be easily controlled. It was also important to keep in mind that the dipping movement produces some shear which may cause issues should cells be incorporated within the fluid. Although testing was done at a maximum of 40 mm/sec, this would likely not have been ideal for cells so further testing was kept within a range of 10-30mm/sec.

3.2.1 Hand Dipping

The most important section of the device is the moving axis which allows for the dipping movement. In the initial rough stages of the project to determine dipping considerations, this was carried out with simple hand dipping. This allowed for easy handling such as changing of speed and positioning for the fiber withdrawal. The process consisted of hand dipping the fiber into the alginate then moving the fiber up and away from the fluid container to allow the droplets to form before spraying the calcium chloride crosslinking agent on the droplets. During this initial dipping it was found that the fiber positioning was important for achieving a consistent final droplet shape. When the dipped fiber was positioned horizontally, the droplets adopted a clam-shell shape while a vertical positioning caused barrel shaped droplets. The disadvantage to hand dipping was the lack of a consistently reproducible speed that could be used for tuning the process. This led to the need to make use of a device with a programmable moving z-axis.

This first experiment was also used to determine the type of fiber material that would be ideal to use for the dipping process. Various fibrous materials were tested such as cotton thread, silk thread, metal wires, and PLA. It was determined that soft fibers such as cotton and silk would not be ideal as they absorbed the fluid and also had issues keeping straight during the dipping process. The metal and PLA fibers were found to work best due to their stiff structure. These

materials were also found to have the advantage of being available at different diameters which would allow for more control over the droplet sizes.

3.2.2 Automated Dipping- Fiber Movement

The next step for the creation of the dipping device was to have a programmable dipping arm which would be able to dip the fiber at a controlled reproducible speed. For this, a 3D printer was repurposed since the machine already had the ability to be programmed for movement along an axis. Placing the 3D printer on its side allowed for controlled positioning along the z-axis. The device was programmed to be able to lower the fiber into the fluid then pause for a set length of time before lifting to withdraw the fiber, allowing the fluid to coat the fiber. Once the withdrawal was complete the process would finish and allow for the coating on the fiber to form the droplets.

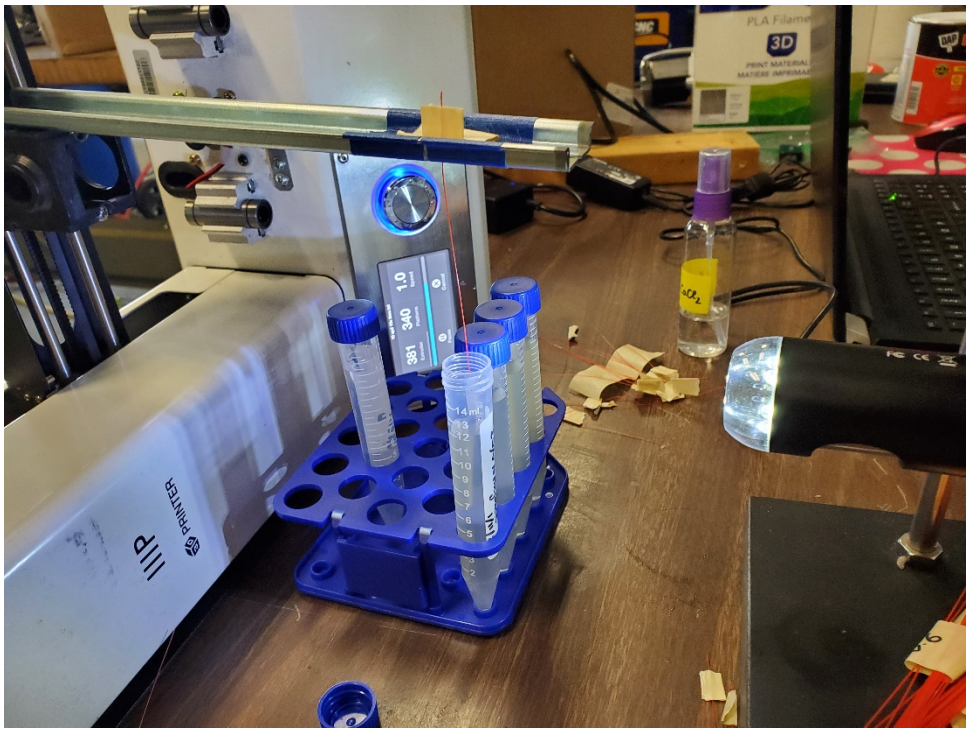

Figure 3.1: The original setup which used the 3D printer axis consisted of a roughly attached metal bracket. A slot in the bracket was covered with tape to create a slit for the PLA fiber to pass through. Masking tape was added to the upper end of the fiber to allow it to hang from the bracket arm.

The assembly consisted of a metal bracket attached to the moving axis of the 3D printer as shown in Figure 3.1. The initial holder for the fiber was simple hole initially made from tape

with a stopper added to the top the fiber for consistent fiber dipping length. However, this holder was not stable and led to inconsistent fiber positioning, so an alternative fiber holder was created using a syringe with a needle attachment and Play-Doh as shown in Figure 3.2. The use of the Play-Doh in combination with the needle tip syringe was meant to keep the fiber in place and contain as much of the fiber as possible to dampen any vibrations from external sources. This holder was found to work well to increase the consistency of the fiber positioning and keeping the fiber stable during the dipping process. The use of the arm to dip the fiber allowed for better control over the tuning of the process, however it was found that the movement of the fiber created vibrations which led to complications with the stability and imaging of the droplets.

3.2.3 Automated Dipping- Sample Movement

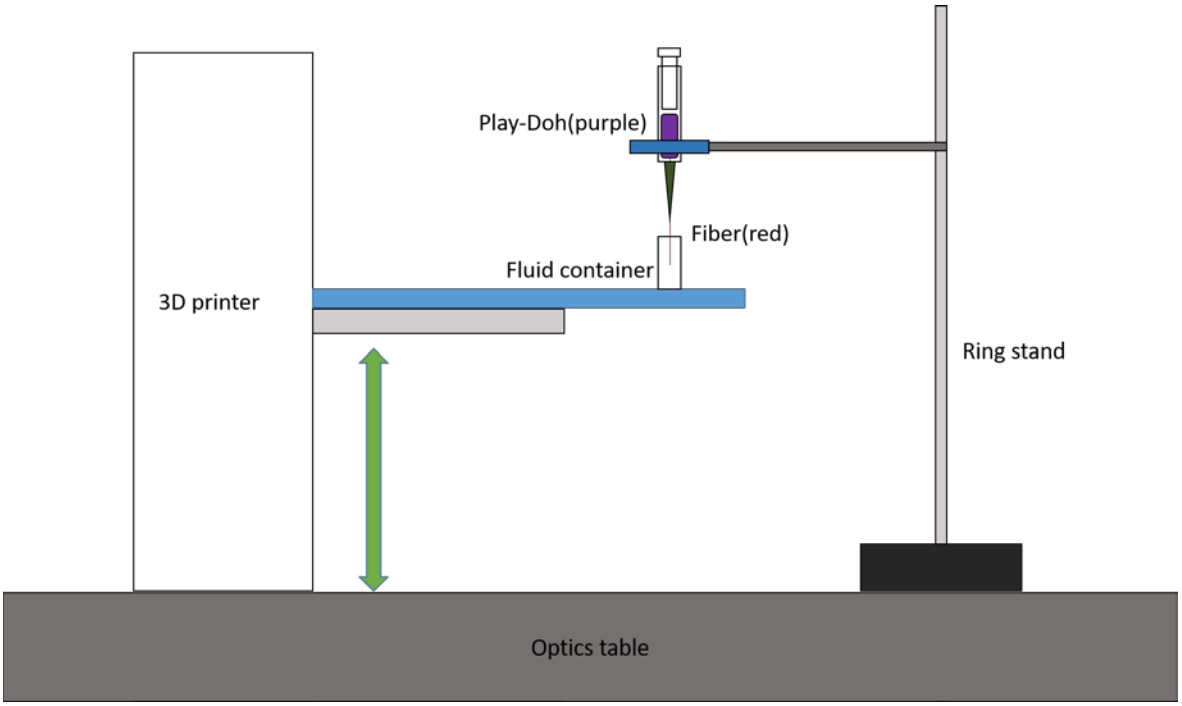

Figure 3.2: Changed setup for the dipping process where the fiber is stationary to avoid vibrations and the fluid container moves along the z-axis. The setup location was on an optics table which allowed for specific positioning of the set-up components.

Since the fiber vibrations were caused by the mechanical movement of the machine, a change was made to make the fiber stationary while the fluid container would be moving along the z-axis as shown in Figure 3.2. This meant that the arm which was originally holding the fiber

needed to be changed to a stage to hold the fluid container. The original metal bracket arm did not have the stability or the level platform needed to hold the fluid. So, black acrylic was rigidly screwed on to the 3D printer to create a flat, level platform. The moving stage was tested comparing a narrow stage with a wider and slightly thicker stage. The latter was found to have issues with moving down the z-axis possibly due to its larger mass relative to the smaller stage so the wide stage may have been closer to the maximum capacity that the printer set-up could handle. Once the stage seen in Figure 3.3 was finalized, the coding for the axis movement needed to be altered since this setup would change the direction of the printer movement. The original coding was for the fiber to move down into the fluid then be lifted out while the changed setup moved in the opposite direction with stage moving up towards the stationary fiber then back down to withdraw the fiber from the fluid.

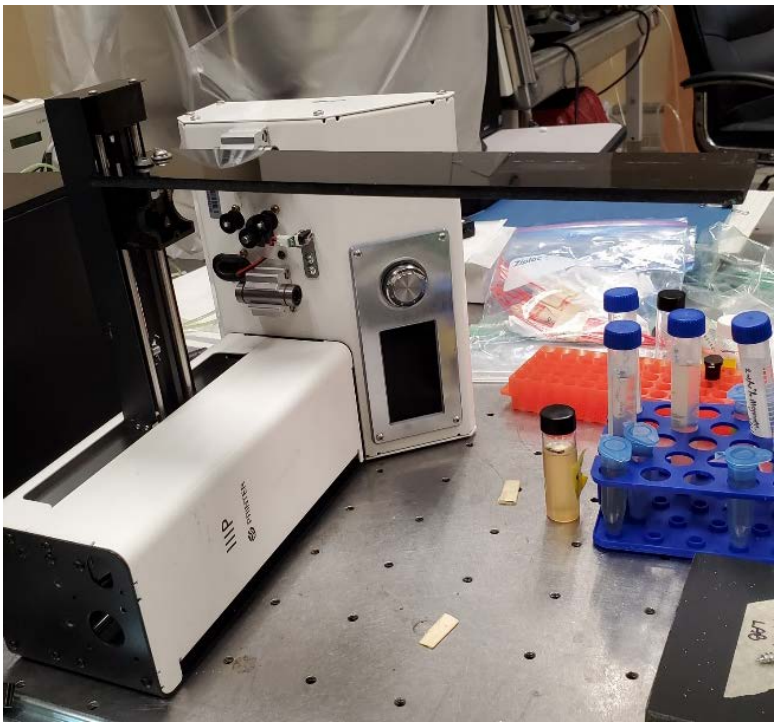

Figure 3.3: Final decided stage for the fluid container movement.

Another characteristic that needed to be determined was the ability of the stage to hold the fluid in place. During this time the volume of the container was not fully decided and so the stage needed to be able to accommodate whichever containers were to be tested. The acrylic

stage was a simple platform but had no edges that could keep a container in place during the dipping process. For this, the covers of 50ml and 15ml centrifuge tubes were glued to the acrylic arm as a set base while the bottoms of the tubes were cut then screwed onto the glued caps as shown in Figure 3.4. This created a holder for the fluid container to be kept during the dipping process. At the time of this development the fluid container was being compared so the holder needed to be used for various sizes.

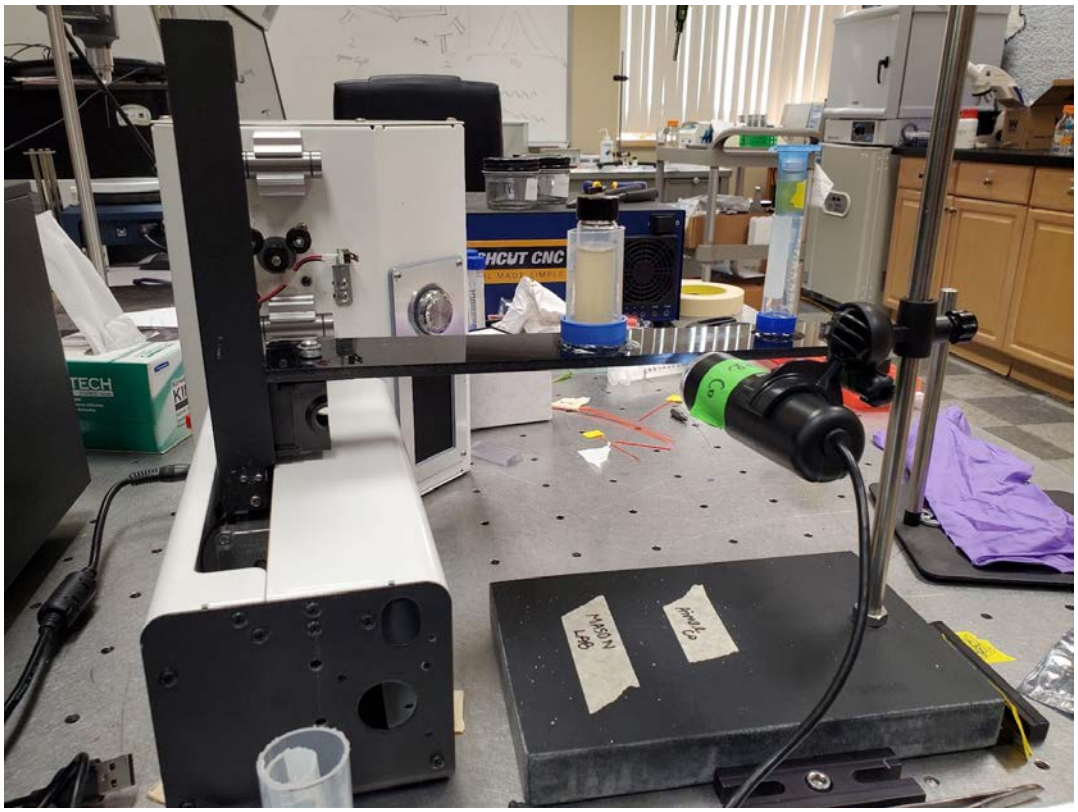

Figure 3.4: Setup for the testing of different fluid containers for the dipping process. A disposable 50ml and 15ml centrifuge tube were used to attach the fluid containers to the acrylic arm. The caps of both centrifuge tubes were glued to the acrylic and the closed ends of the tubes were cut off to create an open holder for the fluid container. Gluing the caps rather than the entire centrifuge tube allowed for easy removal whichever container was not in use.

3.3 Fluid Containment

The initial container that was used for the hand dipping was a 40ml glass vial. The initial tests seemed to work well with this container however it was realized that the ideal dimensions for the cells to be contained in the droplets would require a fluid container of a smaller diameter. For maximum cell containment within the droplet, an ideal setup would use a small fluid volume

to increase the cell concentration while a small container diameter would place the cells suspended in the fluid closer to the fiber and cause more cells to be drawn up into the fluid coating the fiber.

The next container tested was with 15ml centrifuge tubes as these were of a smaller diameter than the 40ml glass vials. As these were tested when the set-up consisted of a stationary fluid and moving fiber, this container had the advantage of being plastic and could be stored in a centrifuge tube rack for easy storage and transportation. These tubes had a smaller diameter but were also long and so were thought to not be ideal for withdrawing the maximum about of cells during the dipping process.

Two alternate containers were simultaneously considered and compared while altering the dipping setup for a moving fluid container and stationary fiber as shown in Figure 3.4. A 5mL microfuge tube with a 12.63mm opening and a short 15ml glass vial with an 8.2mm opening were tested and compared.

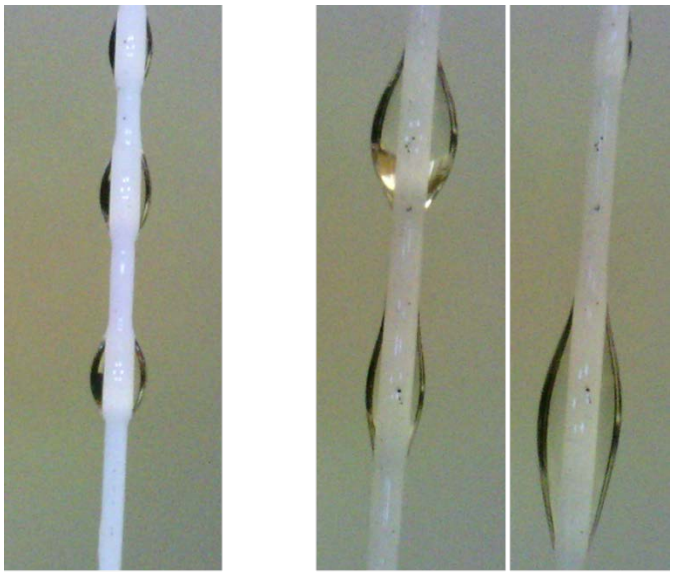

Figure 3.5: Example of droplet resulting from dipping using different containers. The glass vial was found to produce a greater number of smaller and more consistent droplets. The plastic tube created droplets of a larger size which would quickly combine and often drop off the fiber.

All other parameters such as the fiber characteristics and dipping speed were kept constant and the resulting droplets were observed as shown in Figure 3.5. When the fiber was dipped into the plastic tube, the droplets formed were inconsistent in size and not stationary as they would quickly combine and eventually drop off the end of the fiber. The use of the glass vial formed a larger quantity of droplets which were more consistently sized and while they would still eventually combine, it took a longer time than with the plastic tube.

After various testing, the decided fluid container was the 15ml glass vial. Although the 5ml microfuge tube was comparatively smaller and would use less volume to increase the cell concentration, the shorter height of the container resulted in fewer droplets (<10) formed in comparison to the glass vial (10<). It should be noted that more exploration of this may be needed as the containers were of different materials with vastly different opening measurements. Revisiting these tests with containers of the same material and a more gradual range of sizes would allow for more concrete knowledge on the ideal fluid container for the device.

3.4 Fluid Characterization

Once the components of the dipping device were determined, the next important parameter to consider were the characteristics of the dipping fluid. Characterization of the alginate solution was done through rheological testing to determine the flow behavior, which was important since the fluid characteristics determine the resulting flow from the dipping process to form the droplets on the fiber. Compared to a viscometer which can only determine viscosity using rotational test, rheometers can determine more parameters by operating with continuous rotation or rotational oscillation to run shear and torsional tests. The absolute measuring system of the rheometer is obtained through following specific standard measuring geometries, each suitable for specific types of fluids[26].

The rheometer uses torque to record the shear force and calculates the shear stress using the known shear area of the measuring system. In addition, the shear rate is recorded using the rotational speed velocity and the shear gap. The characterization of the alginate fluid was done

using Anton Parr MCR 302e rheometer using the parallel plate geometry measuring system and a 1mm gap at room temperature (25°C). Fluid viscosity values are not constant since they can be affected by various conditions. For this reason, flow behavior is often represented as either a flow curve or viscosity curve. A flow curve is a diagram which presents the shear stress and the shear rate with the latter usually plotted on the x-axis while a viscosity curve presents the viscosity with the shear rate or shear stress on the x-axis. The biggest changes in viscosity are mostly seen within the range of low shear rates so these diagrams are often plotted on a logarithmic scale to better illustrate these values together with the larger shear values.

The flow curves were determined for each alginate concentration and confirmed that the alginate fluids were non-Newtonian as the fluid viscosity was dependent on the shear rate that the fluid experiences. Two different analysis methods, the Power Law method and Carreau-Yasuda method, were explored for the determination of the flow curve equation which was needed to calculate the dipping viscosity. The Power Law model makes use of the power law equation:

$$\eta = K \cdot \gamma^{n-1}$$

where η is the viscosity, γ is the shear rate, K is the flow consistency index, and n is power law constant. This is the simplest model for non-Newtonian fluid as it uses a two-parameter expression to describe the viscosity curve over the linear portion of the log-log plot. Both K and n are constants which characterize the fluid and n-1 is the slope of the logη vs logγ plot.

The use of only two fitting parameters makes the power law model the simplest of the non-Newtonian models but is not always the best curve fit for most data[27].

The Carreau-Yasuda Model uses a five-parameter equation and is the generalized form of the power law equation:

$$\eta := \eta_0 \cdot \left[1 + (\lambda \cdot \gamma)^a\right]^{\frac{n-1}{a}}$$

where η_0 is the zero-shear viscosity, λ is the time constant which determines where it changes from constant to power law, γ is the shear rate, a is the variable which affects the shape of the transition region, and n describes the slope of the power law.

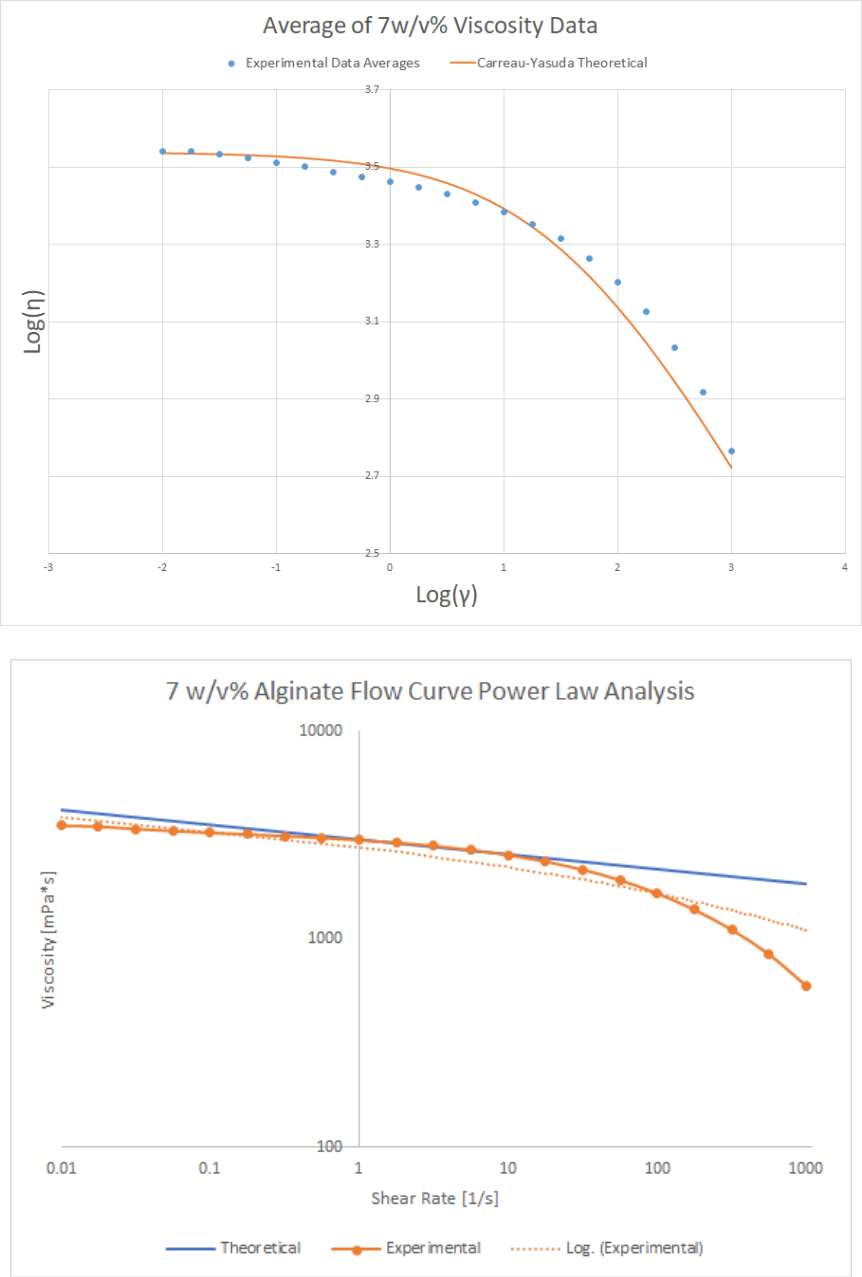

Figure 3.6: Comparison of two different non-Newtonian fluid models, the Power Law Model and the Carreau-Yasuda Model.

The comparison of the two plots in Figure 3.6 shows that the Carreau-Yasuda model shows a better fit for the overall experimental data. However, it was noticed that the linear portion of the experimental data seemed to fit better to the power law model over the Carreau-Yasuda model. The shear rate for each dipping speed was calculated to determine the range of shear rates tested on the alginate fluid.

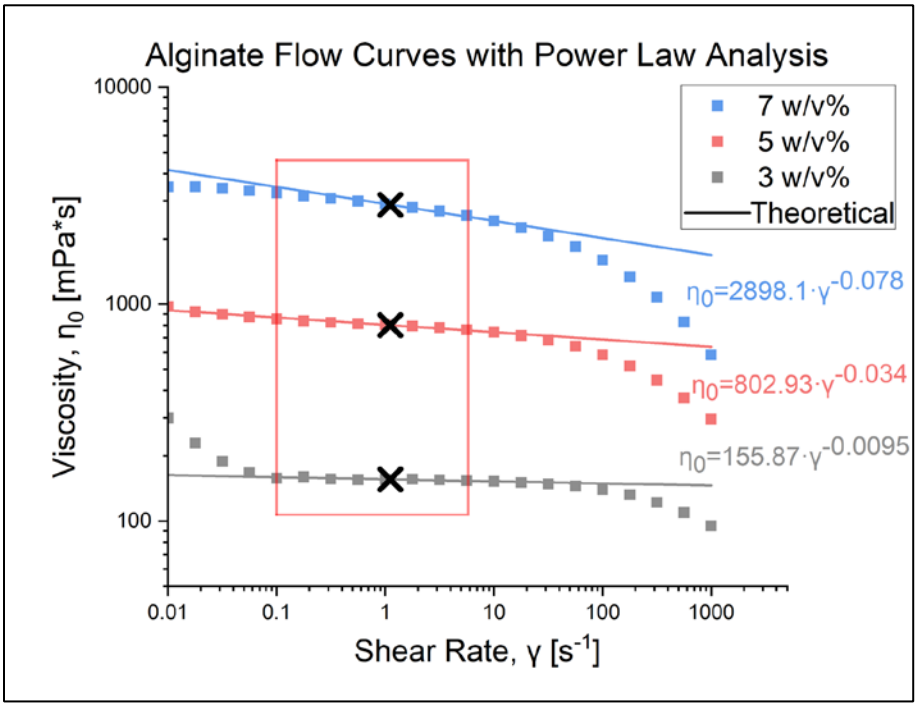

Figure 3.7: Flow curves for different alginate concentrations

This range fell in the linear section of the flow curve which confirms that the viscosity was able to be calculated through using the Power Law Equation. The final speed of the dipping process at 10mm/s gave a shear rate for the insertion of the fiber to be 1.116s^{-1} which is indicated on by the X in Figure 3.7. The calculated viscosity values from the use of Power Law are presented in Table 3.1.

Table 3.1: Characterization of the alginate dipping fluid

Alginate Concentration, % [w/v]	Viscosity, η [mPa*s]	Density, ρ [g/mL]	Contact Angle, θ [°]
3	155.71	1.011	26.74
5	799.96	1.018	50.52
7	2873.29	1.025	62.55

The rheometer is also capable of recording the time dependent behavior of the fluid using three-interval thixotropy tests (3ITT). This is a rotational test consisting of three intervals: 1) A period of very low shear to simulate behavior at rest. 2) A period of strong shear to simulate structural breakdown. 3) A period of low shear to simulate structural regeneration at rest. 3ITT tests were done on the rheometer to look at the viscosity recovery of the alginate fluids after experiencing shear. These tests, shown in Figure 3.8, were done with 1 w/v%, 3 w/v%, 5 w/v%, and 7 w/v% alginate as this was the initial full range of alginate concentrations being tested. However, 3ITT testing of the 1 w/v% alginate and 3 w/v% alginate were inconclusive. This may have been due to the resulting measurements being too low for the rheometer to read. The successful 3ITT tests showed that the fluids were able to recover well over time and would have likely returned to the original viscosity if measured for a longer amount of time. These tests were taken as they may be necessary for the deciding dwelling time in the dipping process which is when the fiber is paused between the dip and withdrawal step. These results combined to the knowledge from the flow curves of the viscosity during the dipping shear brought the decision that the dwelling time did not need to be exceedingly long. The viscosity change during the dipping shear is significantly less than that experienced during the 3ITT testing so the recovery was expected to be much faster.

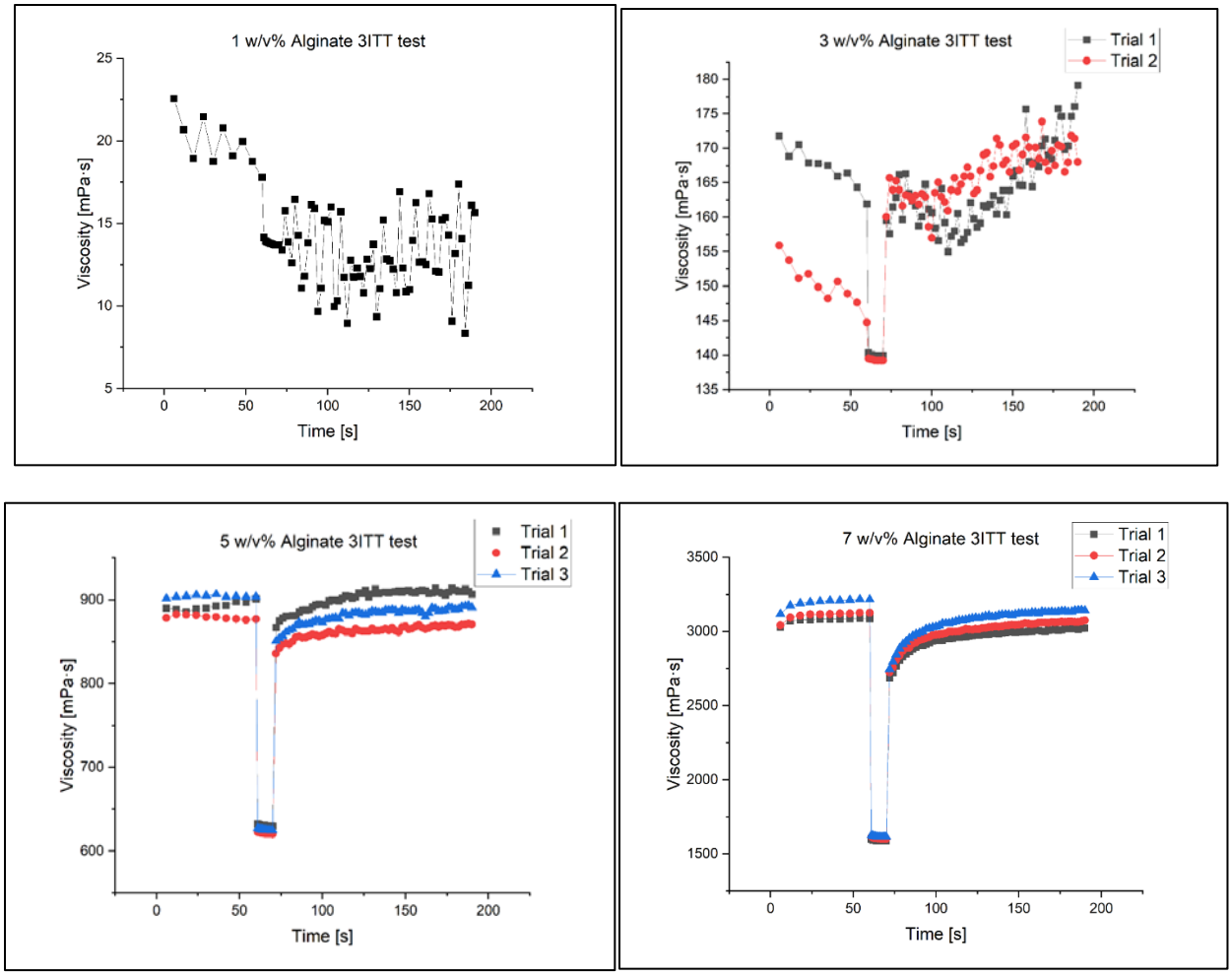

Figure 3.8: 3ITT tests done with the 1 w/v% alginate, 3 w/v% alginate, 5 w/v% alginate, and 7 w/v% alginate.

3.5 Final Dipping Process

The last parameter needed to determine the final dipping process was the dipping speed which refers to the speed of which the fiber enters and withdraws from the fluid. Dipping speeds between 1mm/s and 40mm/s were tested using 0.3mm and 0.2mm diameter PLA fibers. The lower speeds were found to be too slow for any coating formation and so no droplets were formed. The lowest dipping speed that was able to form droplets was 10mm/s and testing continued at increasing speeds up to 40mm/s as shown in Figure 3.9. For each trial, the fiber was dipped and withdrawn at the set speed and the initial number of droplets formed was counted and then recounted after individual droplet imaging was completed. The imaging process with the digital

microscope camera allowed for imaging along the fiber and required manual movement of the camera along the ring stand. After the imaging was complete the number of droplets was recounted and recorded as the final number of droplets after any droplets had evaporated or combined. The decision for the ideal dipping speed needed consideration for the droplet size as well as the number of droplets. The higher speeds were able to coat the fiber easily however the increased speed caused a thick coating which was still able to break off into droplets but these droplets were extremely large and would quickly drop off the end of the fiber back into the fluid container.

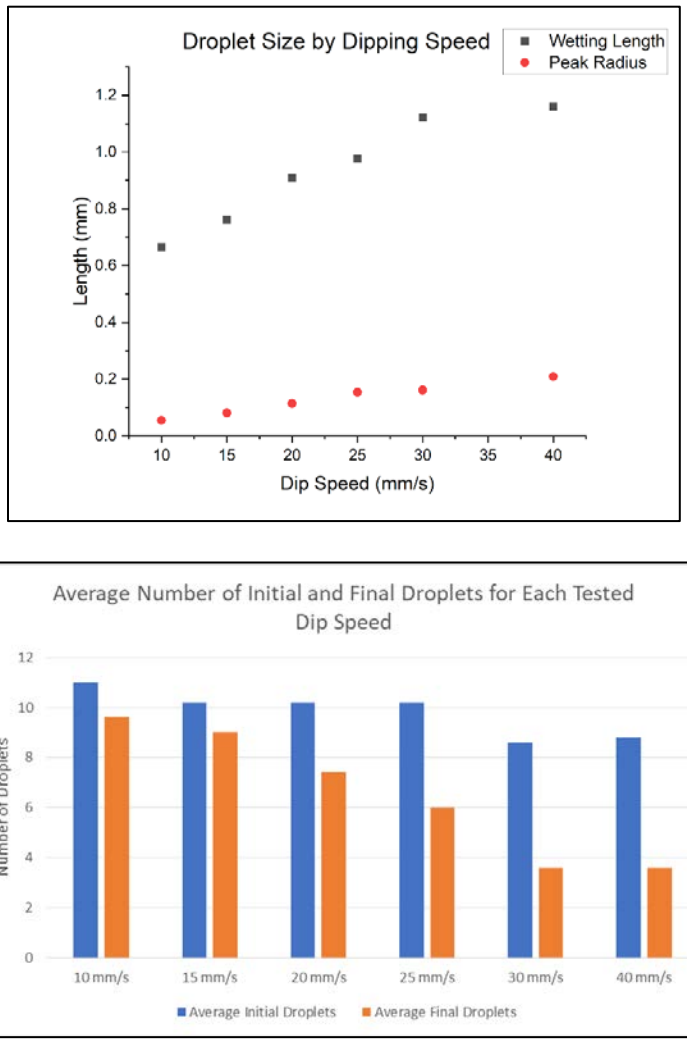

Figure 3.9: Results from testing the droplet formation with different dipping speeds. The increase of speed caused larger droplet to form but also resulted in fewer droplets during both the initial and final droplet count.

The speed that produced and retained the largest number of droplets was found to be 10mm/sec using a 0.2mm fiber and so was chosen as the set speed parameter as shown in Figure 3.10. Between the fiber submersion and withdrawal there is a period of time during which the fiber is stationary within the fluid, which is called the dwelling time. This was necessary to allow for the fluid to return to its zero-shear viscosity before fiber removal. This time was kept fixed at 10 seconds as the current parameters in use did not appear to be heavily influenced by the dwelling time. With all of the parameters for the physical dipping process optimized, quick dipping tests were carried out to identify the time needed for full droplet formation for ideal imaging, which was found to be 2 minutes.

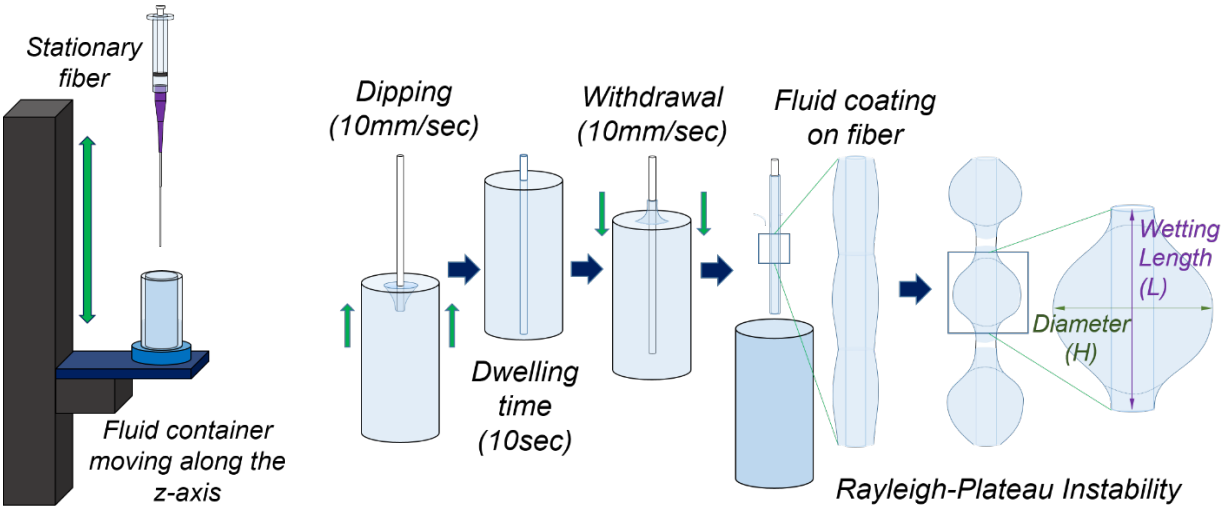

Figure 3.10: The final dipping process consisted of a stationary fiber with a container of fluid moving upward to at 10mm/sec to submerge the fiber. There is a dwelling time of 10 seconds to allow for the fluid to properly surround the fiber and return to the zero shear viscosity. Once the dwelling time is complete, the fluid container moves down to allow the fiber to withdraw and form the fluid coating required to induce droplet formation by Rayleigh-Plateau Instability.

3.6 Imaging

Along with the various changes to the dipping set-up itself, the imaging process also changed. For imaging during the initial hand dipping tests, a Samsung Galaxy S10+ phone camera was used. The camera was used in Pro Mode which gave the ability to alter settings similar to those of a DSLR camera. Setting the focus to manual and using macro mode, allowed

for clear images of the entire fiber while being able to use digital zoom to measure the individual droplets. After the fiber was hand dipped, the setup shown in Figure 3.11 was used to position the phone at the correct height and distance from the fiber for the imaging.

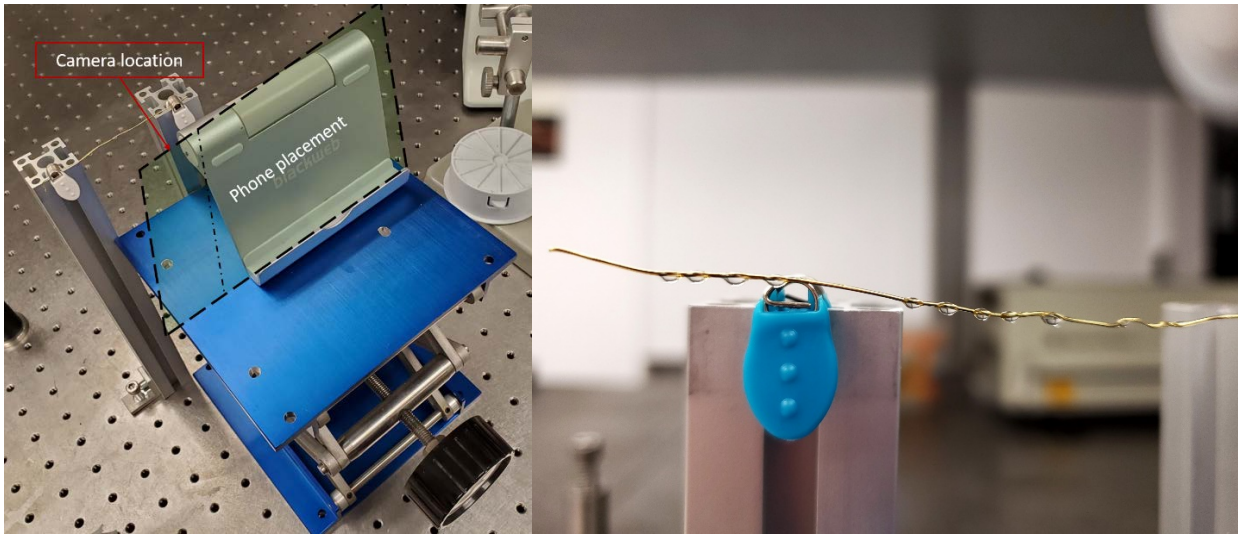

Figure 3.11: The image on the left of the figure shows the setup for the immediate imaging of the fiber after the dipping process. With this setup, the fiber was hand dipped into the fluid with the dry end already clipped and then quickly placed on the T-slot extrusions screwed onto the optics table. The image on the right shows an example image obtained through this set-up

Although the phone camera was able to take clear pictures of the droplets on the entire fiber, this was not ideal for the magnification required to analyze the individual droplets. The transition from hand dipping the fiber to the use of the 3D printer arm also brought about another problem with the use of the phone camera. To get the manual focus to work for the phone, the lens needed to be a specific distance from the fiber which could not be achieved using the previous stage and phone stand. When the setup was changed to use the 3D printer arm, various camera types were explored as shown in Figure 3.12.

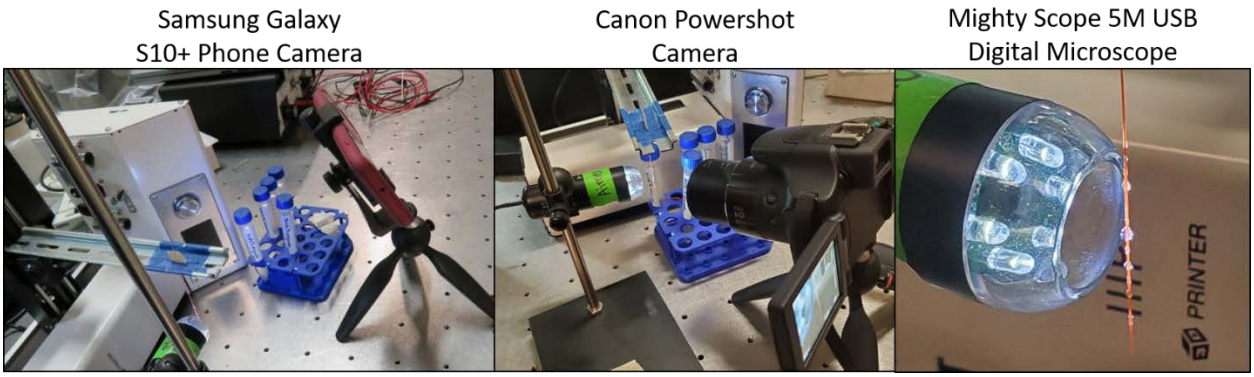

Figure 3.12: Different camera options explored when moving from the hand dipping setup to the 3D printer arm set-up.

The Canon Powershot Camera gave better quality images in comparison to the phone camera, however the bulky size of the camera caused difficulty with operating the 3D printer setup. Using the Mighty Scope 5M USB Digital Microscope improved the quality of the imaging along with the improved ease of use in regards to the positioning of the camera. The phone camera was limited by the positioning of the stage and phone stand while the microscope camera had the ability to be attached to ring stand. This gave the advantage of easy adjustment along the z-axis as well as x-y positioning around the fiber. Comparing the images produced by the different camera in Figure 3.13, the microscope camera provided the best magnification for accurate measurements of droplets.

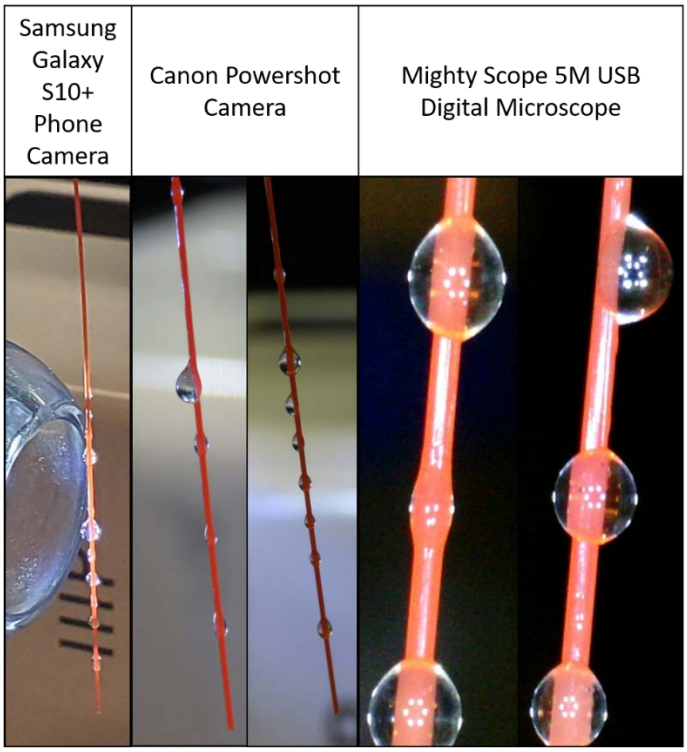

Figure 3.13: Examples of images obtained when testing the different types of cameras.

3.7 Image Analysis

The image analysis process changed over the development of the overall dipping process due to changes such as image quality and material coloring. The initial analysis process on ImageJ made use of steps such as channel splitting and image thresholding, facilitated by the use of a red PLA fiber. However the light from the camera bouncing off of the droplets caused some problems with imaging due to the reflections so the fiber color was changed to white and a white backdrop was added. This change was also done to help with the contact angle measurement as the use of the white fiber and backdrop provided the necessary greyscale contrast to distinguish between the droplet and fiber. Although this created better quality images and helped with contact angle measurement, the analysis was unable to use the same methods to measure droplet dimensions. With these changes, the easiest method for the droplet measurement was manually measuring them on ImageJ (shown in Figure 3.14) while using the known fiber diameter as a scale for the measurements of the droplet diameter and wetting length.

Additional measurements of the contact angle were also taken at this time for the characterization of the dipping fluid using the Drop Analysis-LB-ADSA Plugin.

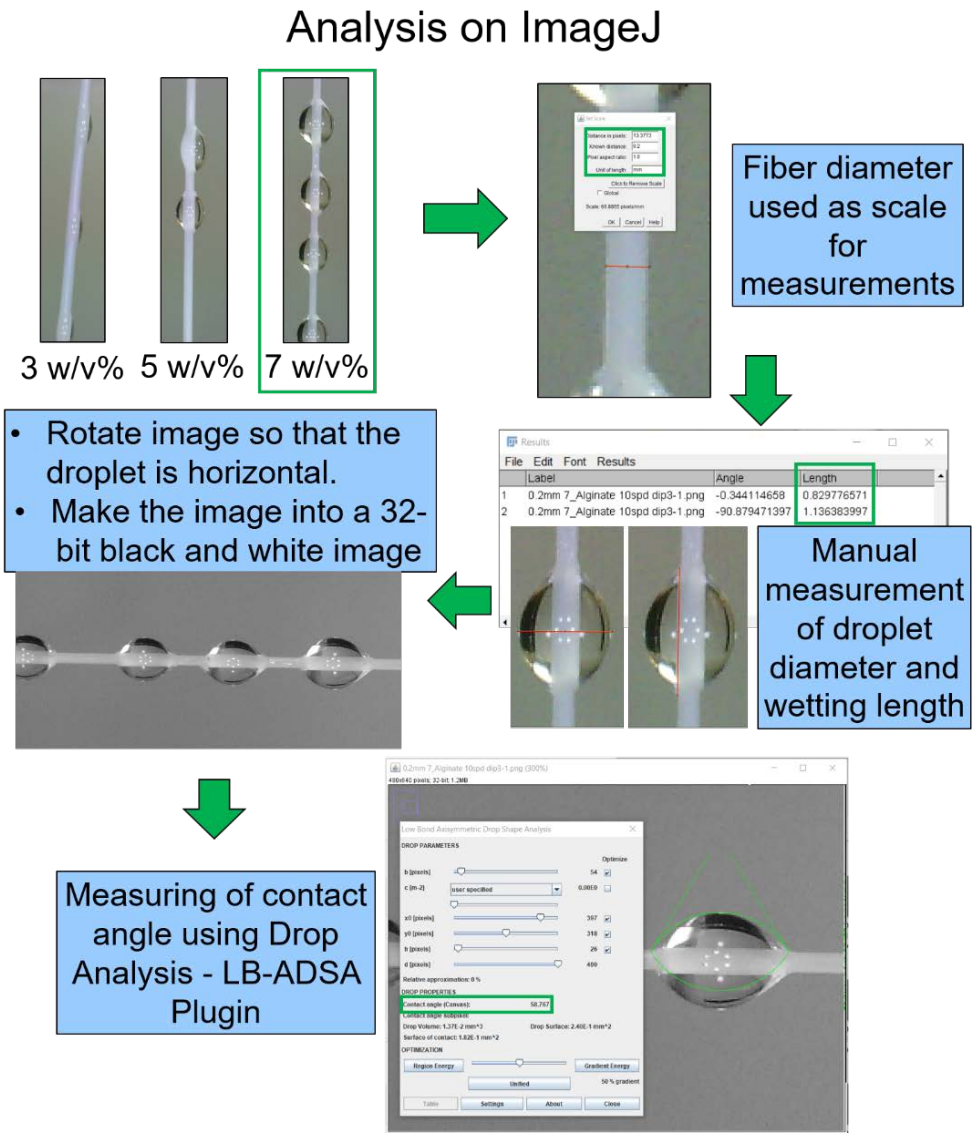

Figure 3.14: The steps of the analysis process for the droplet images. The imaging process required the camera to be moved during the dipping process so a scale bar would need to be redone each time the camera moved. To avoid this, the diameter of the fibers were measured beforehand and then used as the scale for measurements.

3.8 Results

The droplets formed during the dipping process were characterized through an analysis of the droplet shape fidelity and reproducibility. These were evaluated as a function of the dipping fluid composition. The desired spheroid range found in literature was found to be between 300µm and 500µm and so these values were used as a goal for this testing [3, 4, 11, 12]. The shape

fidelity of the droplet can be quantified by the H/L aspect ratio using the droplet diameter (H) and the wetting length (L) as shown in Figure 3.7. This aspect ratio can range between 0-1, where 1 represents the desired perfect sphere. All trials were taken in replicates of three from which the average values were calculated.

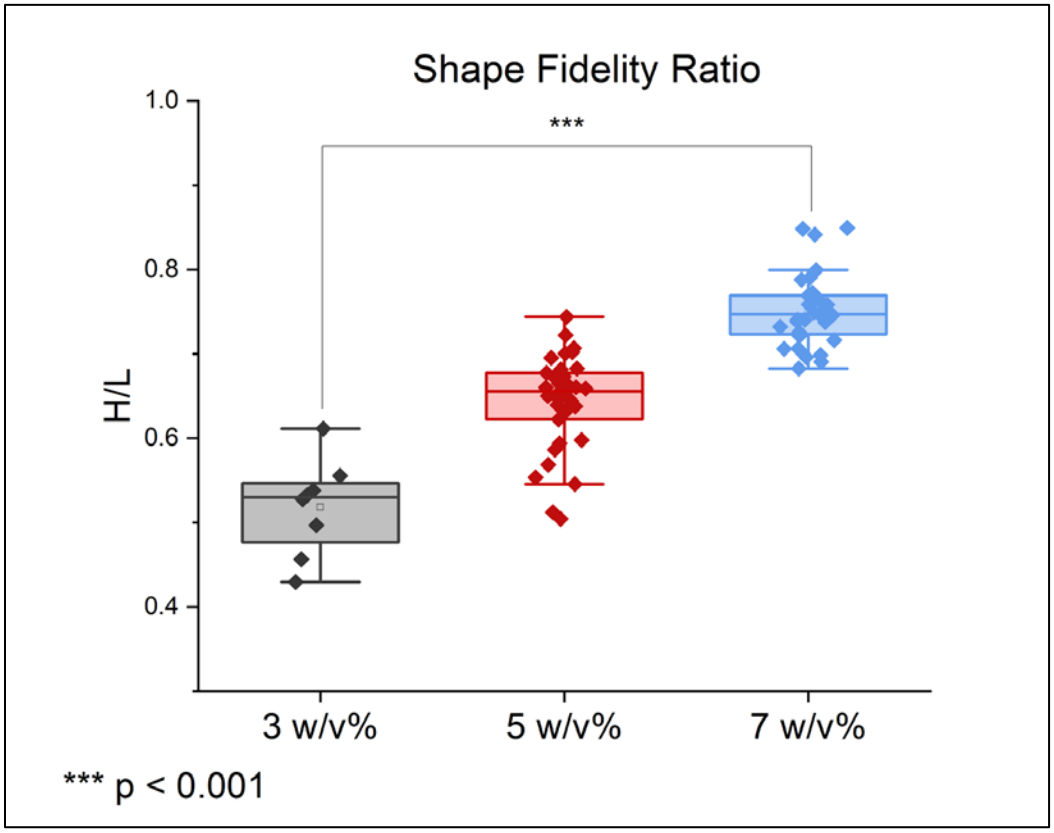

Figure 3.15: Plot to show the change in the droplet shape fidelity between the different alginate concentrations using 2mm fiber and a dipping speed of 10mm/s

A box-whisker plot was used to compare the resulting droplet shape fidelity ratios from dipping with three different alginate concentrations as shown in Figure 3.15. For these tests, other parameters such as dipping speed, fiber diameter, and dwelling time were kept static. As the goal was to form droplets with a shape fidelity close to 1, these results show 7% alginate produced the most spherical droplets.

Table 3.2: Resulting droplet dimensions using different alginate concentrations

Alginate Composition, % [w/v]	Average Diameter, H [μm]	Average Wetting Length, L [μm]	Average H/L Ratio
3	419.5	817.2	0.518383 ± *0.053463*
5	470.5	713.3	0.642574 ± *0.055874*
7	815.2	1082.1	0.751375 ± *0.041926*

These results show that increased alginate concentration led to improvement in the shape fidelity of the droplets. The average values of the droplet measurements presented in Table 3.2 show a clear difference in the droplet sizes caused by the different alginate compositions.

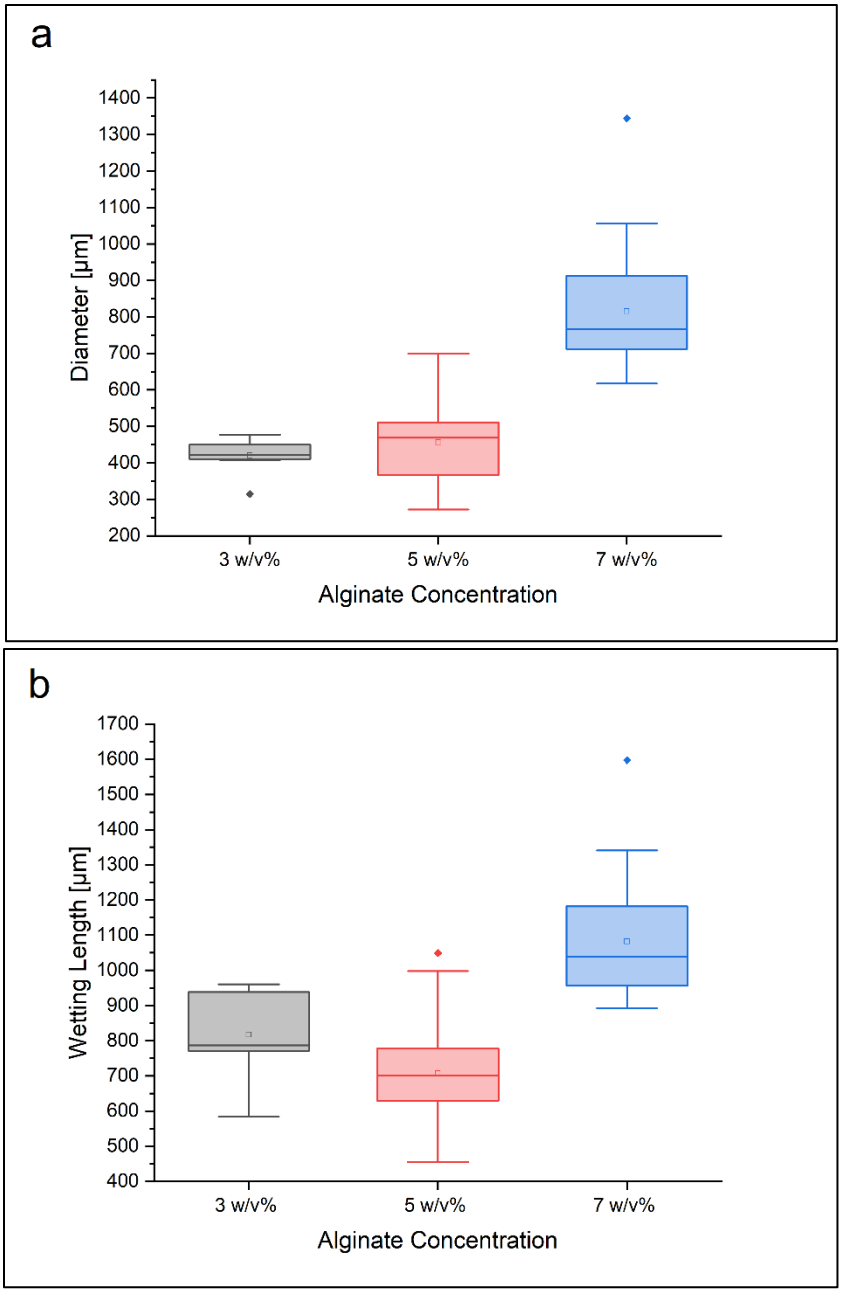

Figure 3.16: Box charts comparing the change in droplet diameter (a) and wetting length (b) for the different alginate concentrations.

The shape fidelity ratio appears to take a linear increase with the increase of alginate concentration. In Figure 3.16 the measurements of the diameter and wetting length each are compared and while the 3 w/v% and 7 w/v% show a wide difference, the comparison of the 3 w/v% and 5 w/v% was shown to decrease in wetting length while overlapping in diameter. For

this reason the preferred characteristic quality of the droplets should be the aspect ratio as the shape of the droplets is an important consideration towards the reproducibility.

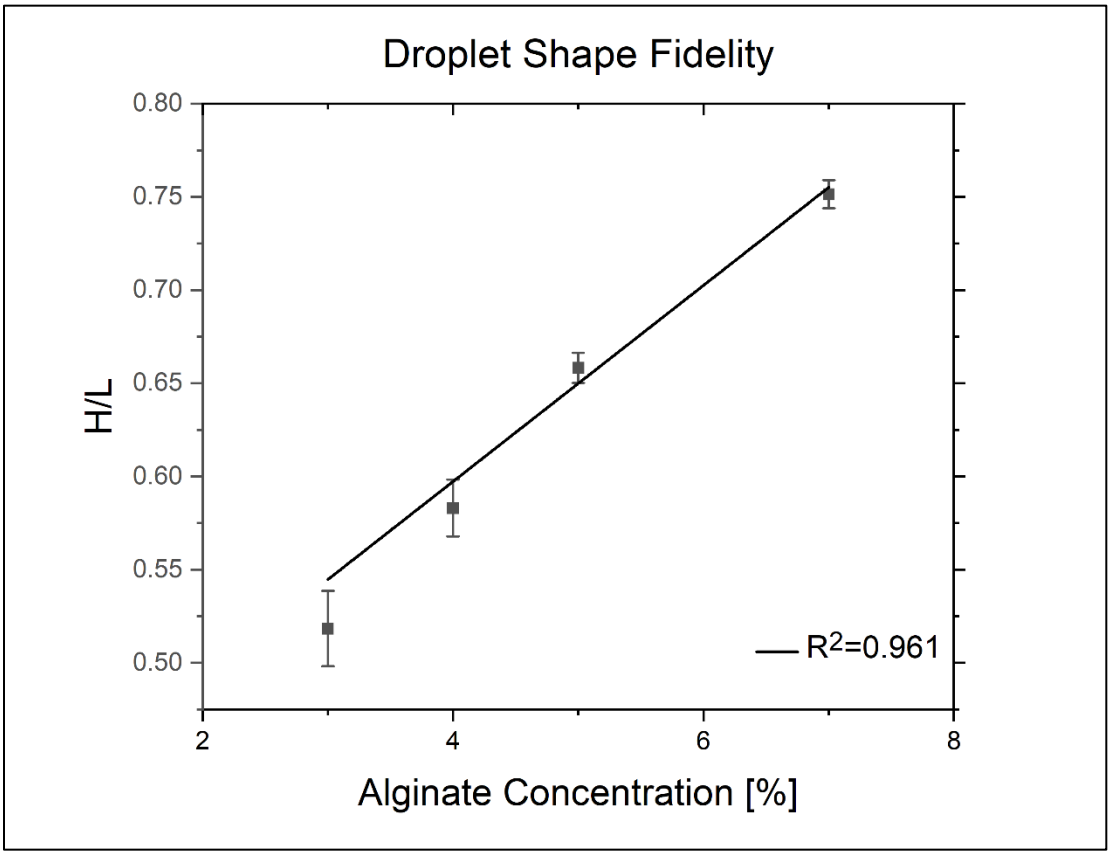

Figure 3.17: Plot showing the relationship between the droplet shape fidelity (H/L ratio) and the alginate concentration. This includes additional data for 4 w/v% alginate which was taken after all other testing. This data is not used for the fitted linear curve

Of the different alginate concentration tested the 7 w/v% was found to produce the most consistently sized droplets with the highest shape fidelity ratio. This is confirmed by the values previously presented in Table 3.2 where H/L≈0.75 with the lowest standard deviation. The resulting trends of the droplet shape fidelity were plotted and shown in Figure 3.17. An additional test with 4w/v% alginate was done and confirmed to follow the expected trend for the H/L aspect ratio.

3.9 Conclusions and Future Directions

In this project, a controlled fiber dipping system was successfully designed which was able to provide consistent results. Tests were done to check the influence of the dipping fluid composition on the resulting droplet shape fidelity and reproducibility. These tests found that the 7w/v% alginate produced the most consistent droplets with the highest shape fidelity ratio showing they were the closest to the ideal of a spherical droplet. Although these droplets were found to be on the larger end of the desired size range, future tests with more focus on the dipping speed can be carried out since previous data showed this to have influence on the droplet size. The trend found relating the droplet shape fidelity to the alginate concentration was confirmed through additional testing of 4 w/v% alginate.

The future work of this project should focus on additional components used in the dipping fluid. The current dipping fluid consists solely of alginate and since the desired usage of this device is for the formation of spheroids, additional components will need to be added to confirm whether the dipping and droplet formation properties remain the same. The simplest change would be the use of cell culture media rather than DI water for mixing of the alginate fluid. Cell culture media has a viscosity which is very close to that of water and so is unlikely to have any substantial influence on droplet shape compared to the alginate fluid made with DI water. Although this is expected to have similar results to not change much, this should still be tested to ensure that the extra components within media such as salts and added serums. These serums are to support the growth of the cells using ingredients which are likely to effect the fluid viscosity. Another expected change needed to the current testing process is the addition of particles to represent the inclusion of cells. This is what is likely to have the most influence on any changes to the current dipping process since this may affect the dipping fluid viscosity. Ideally, these particles should be around the same size as cells (20μm) and need to be easy to visualize in the fluid. An example of a possible particle to use would be monodispersed standard polystyrene particles which have been used to represent cells in a different study [28].

Another future step would include exploration of the crosslinking aspect of the droplets. The current results focused mainly on the dipping abilities of the alginate solution, however the setup was later adjusted for an additional crosslinking step during which the fiber would get dipped into the crosslinking fluid. These quick tests used 4w/v% calcium chloride since it was the median of the alginate concentrations, and were initially to check if the additional dipping had an effect on the droplet dimensions. The ideal crosslinking concentration would be able to keep the droplet form while still allowing for mobility for the contained cells. Simultaneously this step would include the considerations for the storage of the droplets as they would likely need to be contained within an environment ideal for cells. Once all previous steps have been completed to finalize the ideal process for the full dipping system for spheroid formation, trials will move on to use mammalian cells. Since the cell suspension itself is known to be a shear thinning non-Newtonian fluid, the combination with the alginate solution will greatly change the behavior of the dipping fluid. The resulting alginate-cell suspension viscosity will be highly dependent on the ratio of the alginate solution and the cell density used [29, 30].

REFERENCES

1. Kapalczynska M, Kolenda T, Przybyla W, Zajaczkowska M, Teresiak A, Filas V, et al. 2D and 3D cell cultures - a comparison of different types of cancer cell cultures. Arch Med Sci. 2018;14(4):910-9.

2. Fennema E, Rivron N, Rouwkema J, van Blitterswijk C, de Boer J. Spheroid culture as a tool for creating 3D complex tissues. Trends Biotechnol. 2013;31(2):108-15.

3. Ryu NE, Lee SH, Park H. Spheroid Culture System Methods and Applications for Mesenchymal Stem Cells. Cells. 2019;8(12).

4. Achilli TM, Meyer J, Morgan JR. Advances in the formation, use and understanding of multi-cellular spheroids. Expert Opin Biol Ther. 2012;12(10):1347-60.

5. Edmondson R, Broglie JJ, Adcock AF, Yang L. Three-dimensional cell culture systems and their applications in drug discovery and cell-based biosensors. Assay Drug Dev Technol. 2014;12(4):207-18.

6. Langhans SA. Three-Dimensional in Vitro Cell Culture Models in Drug Discovery and Drug Repositioning. Front Pharmacol. 2018;9:6.

7. Fontoura JC, Viezzer C, Dos Santos FG, Ligabue RA, Weinlich R, Puga RD, et al. Comparison of 2D and 3D cell culture models for cell growth, gene expression and drug resistance. Mater Sci Eng C Mater Biol Appl. 2020;107:110264.

8. Fang Y, Eglen RM. Three-Dimensional Cell Cultures in Drug Discovery and Development. SLAS Discov. 2017;22(5):456-72.

9. Velasco V, Shariati SA, Esfandyarpour R. Microtechnology-based methods for organoid models. Microsyst Nanoeng. 2020;6:76.

10. Bialkowska K, Komorowski P, Bryszewska M, Milowska K. Spheroids as a Type of Three-Dimensional Cell Cultures-Examples of Methods of Preparation and the Most Important Application. Int J Mol Sci. 2020;21(17).

11. Gong X, Lin C, Cheng J, Su J, Zhao H, Liu T, et al. Generation of Multicellular Tumor Spheroids with Microwell-Based Agarose Scaffolds for Drug Testing. PLoS One. 2015;10(6):e0130348.

12. Bartosh TJ, Ylostalo JH. Preparation of anti-inflammatory mesenchymal stem/precursor cells (MSCs) through sphere formation using hanging-drop culture technique. Curr Protoc Stem Cell Biol. 2014;28:Unit 2B 6.

13. Quéré D. Fluid Coating on a Fiber. Annual Review of Fluid Mechanics. 1999;31:347-84.

14. Yang Y, Chen X, Huang Y. Spreading Dynamics of Droplet Impact on a Wedge-Patterned Biphilic Surface. Applied Sciences. 2019;9(11).

15. Song M, Kartawira K, Hillaire KD, Li C, Eaker CB, Kiani A, et al. Overcoming Rayleigh-Plateau instabilities: Stabilizing and destabilizing liquid-metal streams via electrochemical oxidation. Proc Natl Acad Sci U S A. 2020;117(32):19026-32.

16. Wang P, Zhou J, Xu B, Lu C, Meng Q, Liu H. Bioinspired Anti-Plateau-Rayleigh-Instability on Dual Parallel Fibers. Adv Mater. 2020;32(45):e2003453.

17. Gallaire F, Brun PT. Fluid dynamic instabilities: theory and application to pattern forming in complex media. Philos Trans A Math Phys Eng Sci. 2017;375(2093).

18. Haefner S, Benzaquen M, Baumchen O, Salez T, Peters R, McGraw JD, et al. Influence of slip on the Plateau-Rayleigh instability on a fibre. Nat Commun. 2015;6:7409.

19. Eggers J, Villermaux E. Physics of liquid jets. Reports on Progress in Physics. 2008;71(3).

20. Lautrup B. Surface Tension. Physics of Continuous Matter2010. p. 69-81.

21. Charru F. The Rayleigh-Plateau capillary instability. Hydrodynamic Instabilities: Cambridge University Press; 2011. p. 64-7.

22. Abasalizadeh F, Moghaddam SV, Alizadeh E, Akbari E, Kashani E, Fazljou SMB, et al. Alginate-based hydrogels as drug delivery vehicles in cancer treatment and their applications in wound dressing and 3D bioprinting. J Biol Eng. 2020;14:8.

23. Lee KY, Mooney DJ. Alginate: properties and biomedical applications. Prog Polym Sci. 2012;37(1):106-26.

24. Wan LQ, Jiang J, Arnold DE, Guo XE, Lu HH, Mow VC. Calcium Concentration Effects on the Mechanical and Biochemical Properties of Chondrocyte-Alginate Constructs. Cell Mol Bioeng. 2008;1(1):93-102.

25. Arefin AME, Khatri NR, Kulkarni N, Egan PF. Polymer 3D Printing Review: Materials, Process, and Design Strategies for Medical Applications. Polymers (Basel). 2021;13(9).

26. Mezger TG. Applied Rheology With Joe Flow on Rheology Road. 1 ed. Austria: Anton Paar GmbH; 2015.

27. Bird RB, Stuart WE, Lightfoot EN, Klingenberg DJ. Introductory Transport Phenomena: John Wiley & Sons, Inc.; 2015.

28. Wang Z, Belovich JM. A simple apparatus for measuring cell settling velocity. Biotechnol Prog. 2010;26(5):1361-6.

29. Wahlberg B, Ghuman H, Liu JR, Modo M. Ex vivo biomechanical characterization of syringe-needle ejections for intracerebral cell delivery. Sci Rep. 2018;8(1):9194.

30. Y. S, Ryu D, Ballica R. <Biotech Bioengineering - 25 March 1993 - Shi - Rheological properties of mammalian cell culture suspensions Hybridoma.pdf>. Biotechnology and Bioengineering. 1992;41:745-54.

BIOGRAPHY OF THE AUTHOR

Aimee Co was born in Orono, Maine on August 30, 1993. She was raised in Orono and graduated from Orono High School in 2011. She attended the University of Maine and in 2015, graduated with a Bachelor's degree in Bioengineering and a Pre-Med minor. Aimee is a candidate for the Master of Science degree in Biomedical Engineering from the University of Maine in May 2022.